Mechanism of the OH Radical Scavenging Activity of Nordihydroguaiaretic Acid: A Combined Theoretical and Experimental Study

Annia Galano,*,† Norma A. Macías-Ruvalcaba,‡ Omar Noel Medina Campos,§ and José Pedraza-Chaverri*,§

Departamento de Química, División de Ciencias Básicas e Ingeniería, Universidad Autónoma Metropolitana-Iztapalapa, 09340 City, México, Departamento de Fisicoquímica, Facultad de Química, Universidad Nacional Autónoma de México, 04510 Mexico City, Mexico, and Departamento de Biología, Facultad de Química, Universidad Nacional Autónoma de México, 04510 Mexico City, Mexico

Received: December 19, 2009; Revised Manuscript Received: March 24, 2010

The antioxidant nordihydroguaiaretic acid (NDGA) is a plant phenolic lignan originally isolated from the creosote bush (*Larrea tridentata*). It has been shown that NDGA scavenges efficiently hydroxyl radicals (•OH). In the present paper the mechanism by which NDGA scavenges •OH is addressed performing a combined experimental and theoretical investigation. We found that NDGA protects, in a concentration-dependent way, bovine serum albumin and DNA from the damage induced by •OH generated by the Fenton reaction. In addition, the NDGA + •OH reaction is predicted to be diffusion-controlled. The first step of this reaction is proposed to occur mainly by a sequential electron proton transfer from NDGA to •OH generating a neutral radical of NDGA, which after a second oxidation step gives a diradical that after a cascade sequential complex reaction produces a cyclic compound. This cyclic product is predicted to have a UV−vis spectrum very similar to that of NDGA, making its identification by this technique very difficult. The electrochemical studies performed in water support the formation of a cyclic compound (C2) as the main product of the reaction. It is concluded that NDGA can scavenge at least two •OH.

Introduction

Reactive oxygen species (ROS) are formed in vast quantities in living organisms as a result of normal oxygen metabolism. The hydroxyl radical (•OH) is the most reactive ROS, and it can be formed intracellularly by a Fenton-type reaction, by Haber−Weiss recombination, via water radiolysis, or by other radicals created from enzyme reactions.[1–5] •OH radicals can also be produced by ultraviolet and ionizing radiations.[6] ROS, and in particular •OH radicals, are very reactive species that can damage molecules of high biological importance like proteins and DNA. This chemical damage is commonly referred to as oxidative stress, and it has been held responsible for numerous health disorders like cancer,[7] cardiovascular disorders,[8] atherosclerosis,[9] and Alzheimer's disease.[10] Therefore, the study of compounds with free radical scavenging activity is a current and important area of research.

The naturally occurring antioxidant nordihydroguaiaretic acid (NDGA) or 4-[4-(3,4-dihydroxyphenyl)-2,3-dimethylbutyl]benzene-1,2-diol is a phenolic lignan originally isolated from the creosote bush, *Larrea tridentata*, which grows in some desert areas of the southwest United States and northern Mexico as well as in some areas of Argentina.[11] *Larrea tridentata* belongs to the family Zygophyllaceae and also is known as Creosote bush, Larrea, chaparral, greasewood, or gobernadora. Chaparral tea has been used in folk medicine for the treatment of more than 50 ailments including rheumatism, arthritis, diabetes, gallbladder and kidney stones, and inflammation.[11] Some of the beneficial properties of NDGA may be attributed to its antioxidant properties. In fact, NDGA is a potent in vitro scavenger of peroxynitrite, singlet oxygen, hydroxyl radical, superoxide anion, and hypochlorous acid.[12] We have previously reported that NDGA is more effective to scavenge •OH than the following recognized •OH scavengers: uric acid, dimethyl sulfoxide, dimethylthiourea, trolox, and mannitol.[12] The antioxidant effect of NDGA has been observed in renal and hepatic toxicity induced by ferric-nitrilotriacetate,[13] ozone-induced tyrosine nitration in lungs,[12] potassium dichromate-induced nephrotoxicity,[14] and streptozotocin-induced diabetic nephropathy.[15] The inhibition of cytotoxicity induced by *t*-butylhydroperoxide[16] and hydrogen peroxide (H_2O_2)[17] in mammalian cells is also consistent with the antioxidant effect of NDGA. More recently it has been shown that NDGA prevents neuronal damage and oxidant damage induced by iodoacetate in primary cultures of cerebellar granule neurons.[18]

However, the mechanism by which NDGA scavenges •OH has not been elucidated so far. Therefore, the main aim of the present work is to study as many different viable mechanisms as possible and to identify those contributing the most to the free radical scavenging activity of NDGA. To that purpose, a combined experimental and theoretical investigation has been performed. The studied mechanisms are: hydrogen atom transfer (HAT), radical adduct formation (RAF), single electron transfer (SET), sequential electron proton transfer (SEPT), and proton-coupled electron transfer (PCET).

Materials and Methods

Reagents. Bovine serum albumin (BSA), NDGA, ethylenediaminetetraacetic acid disodium salt (EDTA), ascorbic acid, ammonium iron(II) sulfate hexahydrate [$(NH_4)_2Fe(SO_4)_2$], Coo-

* To whom correspondence should be addressed. E-mail: agalano@prodigy.net.mx; pedraza@unam.mx.

† Departamento de Química, Universidad Autónoma Metropolitana-Iztapalapa.

‡ Departamento de Fisicoquímica, Universidad Nacional Autónoma de México.

§ Departamento de Biología, Universidad Nacional Autónoma de México.

10.1021/jp912001c
Published on Web 04/26/2010

massie brilliant blue R, glycerol, sodium dodecyl sulfate (SDS), acrylamide, bisacrylamide, mercaptoethanol, ethidium bromide, bromophenol blue, xylene cyanol FF, ficoll 400, agarose, sodium acetate, potassium chloride ≥99.0%, and phenol:chloroform: isoamyl alcohol solution were from Sigma Aldrich Co. (St. Louis, MO, USA). Chloroform, H_2O_2, and trichloroacetic acid were from Mallinckrodt Baker, Inc. (Phillipsburg, NJ, USA). Electrochemical grade tetrabutylammonium hexafluorophosphate (Bu_4NPF_6) was from Fluka. *N*,*N*-Dimethylsulfoxide (DMSO) was obtained from Aldrich (99.9%; <0.0005% H_2O). Distilled and deionized water was used for the electrochemical experiments. All other reagents were analytical grade and commercially available.

Isolation of Deoxyribonucleic acid (DNA). DNA was isolated as follows. Rat liver (0.125 g) was homogenized in 1 mL of SDS lysis buffer (1% SDS, 10 mM EDTA, 50 mM Tris, pH 8.1) and incubated on ice for 10 min. An amount of 1 mL of phenol:chloroform:isoamyl alcohol (25:24:1) solution was added, and the tube was mixed gently and centrifuged at 12 000*g* for 5 min at 4 °C. The supernatant was recovered, mixed with 1 mL of phenol:chloroform:isoamyl alcohol solution, and centrifuged at 12 000*g* for 5 min at 4 °C. This procedure was repeated again. To eliminate residual phenol, one volume of chloroform was added to supernatant, and the tube was mixed and centrifuged at 12 000*g* for 3 min at 4 °C. The supernatant was placed in a new tube, and DNA was precipitated by addition of 0.1 volumes of 3 M sodium acetate pH 5.5 and 2.5 volumes of 100% ethanol. The tube was mixed, incubated at −40 °C overnight, and centrifuged at 9000*g* for 10 min at 4 °C. The supernatant was discarded, and the pellet was dried at air and dissolved in 50 μL of Tris-EDTA buffer, pH 8.0. DNA concentration was measured at 260 nm in a spectrophotometer Beckman DU-400 (Beckman Coulter, Palo Alto, CA, USA).

•OH-Mediated Degradation of BSA and DNA. Experiments of •OH-mediated oxidation of BSA were carried out by using a metal-catalyzed reaction based on Kocha et al.[19] with modifications. A solution of ascorbic acid (0.8 mM)/EDTA (0.4 mM)/$(NH_4)_2Fe(SO_4)_2$ (0.4 mM) was prepared in 50 mM phosphate buffer, pH 7.4, and BSA and NDGA (0−50 μM) were dissolved in it. The assay was made as follows: In 1.5 mL eppendorf tubes was mixed 250 μL of 1% BSA with 250 μL of the same solution of ascorbic acid/EDTA/$(NH_4)_2Fe(SO_4)_2$ with or without NDGA. The generation of •OH was initiated with the addition of 15 μL of 2% H_2O_2. In the control tube (without the •OH generator system), the H_2O_2 was replaced by water. After 30 min of incubation at room temperature, 250 μL of 20% trichloroacetic acid was added, and the mixture was centrifuged at 2236*g* for 30 min at 4 °C. The supernatant was discarded, and the pellet was resuspended in 500 μL of 0.1 M NaOH. To evaluate the protein damage induced by •OH, the samples were subjected to SDS−polyacrilamide gel electrophoresis. BSA (50 μg) (from resuspended pellet) was mixed 1:1 with loading buffer (10% glycerol, 2% SDS, 25 mM Tris-HCl (pH 6.8), 5% mercaptoethanol, 0.1% bromophenol blue) and heated at 100 °C for 1 min. The protein sample was loaded in a 12.5% polyacrylamide gel and electrophoresed at 100 V. After running, gels were stained with 0.2% Coomassie brilliant blue R for 1 h, destained, and scanned in HP scanner model 2200c (Hewlett-Packard Company, Palo Alto, CA, USA).

Experiments for •OH-mediated oxidation of DNA were performed similarly to •OH-mediated oxidation of BSA assays. Briefly, 38.5 μL of solutions of NDGA (0−50 μM) dissolved in a solution of ascorbic acid (0.8 mM)/EDTA (0.4 mM)/$(NH_4)_2Fe(SO_4)_2$ (0.4 mM) were mixed with 10 μL of DNA solution (1 μg/μL) and 1.5 μL of 2% H_2O_2. In the control tube (without the •OH generator system), the H_2O_2 was replaced by water. After 20 min of incubation at room temperature, the reaction was stopped by addition of 50 μL of loading DNA buffer (0.25% bromophenol blue, 0.25% xylene cyanol FF, and 15% ficoll 400).[20] An amount of 10 μL of this mixture was electrophoresed in 1% agarose gel for 1 h. The gel was immersed in water containing ethidium bromide (0.5 μg/mL) for 30 min, and DNA was visualized under UV light using a UVP transilluminator model White/UV TMW-20 (UVP, LLC, Upland, CA, USA) and photographed using a digital camera.

Computational Details. Geometry optimizations and frequency calculations have been carried out using the M05-2X functional[21] and the 6-311++G(d,p) basis set. Unrestricted calculations were used for open shell systems, and local minima and transition states were identified by the number of imaginary frequencies (NIMAG = 0 or 1, respectively). All the electronic calculations were performed with the Gaussian 03 package of programs.[22] Thermodynamic corrections at 298 K were included in the calculation of relative energies. The stationary points were first modeled in the gas phase (vacuum), and solvent effects were included a posteriori by single-point calculations using the polarizable continuum model, specifically the integral-equation-formalism (IEF-PCM)[23–25] and RADII = UAHF. They have been performed using benzene, DMSO, and water as solvents, to mimic environments of diverse polarity. The absorption spectra have been computed with time-dependent density functional theory (TDDFT) at the B3LYP/6-311++G(d,p) level of theory.

Relative Gibbs free energies in solution have been computed using the Hess law and thermodynamic cycles, explicitly including solvation free energies. For example, for H abstractions from NDGA. The Gibbs free energy of reaction in solution

$$\begin{array}{ccccccc} NDGA_{gas} & + & {}^{\bullet}OH_{gas} & \longrightarrow & NDGA(-H)^{\bullet}_{gas} & + & H_2O_{gas} \\ \uparrow -\Delta G_s(NDGA) & & \uparrow -\Delta G_s({}^{\bullet}OH) & & \downarrow \Delta G_s(NDGA_{(-H)}{}^{\bullet}) & & \downarrow \Delta G_s(H_2O) \\ NDGA_{sol} & + & {}^{\bullet}OH_{sol} & \longrightarrow & NDGA(-H)^{\bullet}_{sol} & + & H_2O_{sol} \end{array}$$

(ΔG_{sol}) can be obtained as the sum of the Gibbs free energy of reaction in vacuum (ΔG_{gas}) and the difference in solvation free energies ($\Delta\Delta G_S$)

$$\Delta G_{sol} = \Delta G_{gas} + \Delta\Delta G_S \quad (1)$$

where $\Delta\Delta G_S$ is calculated as

$$\Delta\Delta G_S = \Delta G_S(\text{NDGA}(-\text{H})^{\bullet}) + \Delta G_S(\text{H}_2\text{O}) - \Delta G_S(\text{NDGA}) - \Delta G_S({}^{\bullet}\text{OH}) \quad (2)$$

with ΔG_S representing the free energies of solvation. In all the cases, the reference state is 1 M. The solvent cage effects have been included according to the corrections proposed by Okuno,[26] taking into account the free volume theory.[27] These corrections are in good agreement with those independently obtained by Ardura et al.[28] and have been successfully used by other authors.[29–35]

The rate constants (*k*) were calculated using Conventional Transition State Theory (TST)[36–38] and 1 M standard state as

$$k = \sigma\kappa\frac{k_B T}{h}e^{-(\Delta G^{\ddagger})/RT} \quad (3)$$

where k_B and h are the Boltzman and Planck constants; $\Delta G^{\ddagger}$ is the Gibbs free energy of activation; σ represents the reaction path degeneracy, accounting for the number of equivalent reaction paths; and κ accounts for tunneling corrections. The tunneling corrections defined as the Boltzmannn average of the ratio of the quantum and the classical probabilities were calculated using the Eckart barrier.[39]

For the mechanisms involving electron transfers (ETs), the Marcus theory was used.[40–42] It relies on the transition state formalism defining the ET activation barrier ($\Delta G^{\ddagger}_{ET}$) in terms of two thermodynamic parameters, the free energy of reaction (ΔG^{0}_{ET}) and the nuclear reorganization energy (λ)

$$\Delta G^{\ddagger}_{ET} = \frac{\lambda}{4}\left(1 + \frac{\Delta G^{0}_{ET}}{\lambda}\right)^2 \quad (4)$$

In this work, a very simple approximation has been made to calculate λ

$$\lambda \approx \Delta E_{ET} - \Delta G^{0}_{ET} \quad (5)$$

where ΔE_{ET} has been calculated as the nonadiabatic energy difference between reactants and vertical products, i.e., $NDGA^{\bullet+}$ and OH^- in the geometries of NDGA and $^{\bullet}OH$. This approach is similar to that previously used by Nelsen and co-workers[43,44] for a large set of self-exchange reactions.

Some of the calculated rate constant (k) values are close to the diffusion limit. Therefore, the apparent rate constant (k_{app}) can not be directly obtained from TST calculations. In the present work, we have used the Collins−Kimball theory[45] for that purpose.

Electrochemistry. Cyclic voltammetry experiments were done using a conventional three-electrode cell, with a glassy carbon working electrode of 0.3 cm of diameter from Bioanalytical Systems and a platinum wire as the counter electrode. For experiments in aqueous solution a Ag/AgCl (saturated KCl) reference electrode was used, while for experiments in DMSO a silver wire immersed in 0.010 M $AgNO_3$/0.10 M Bu_4NPF_6/acetonitrile served as the reference electrode. In DMSO, the potential of this reference electrode was measured vs the potential of the ferrocenium/ferrocene couple in the solvent being studied, and all the potentials are reported vs ferrocene. For the experiments in water the potentials are reported vs Ag/AgCl. The highly polished glassy carbon electrode was repolished before use with 0.05 μm alumina paste (Buhler), rinsed with water, and sonicated for 5 min in water. It was then rinsed with acetone and dried with a tissue. Voltammograms of NDGA were recorded at room temperature in two different media, 1.0 M KCl and 0.1 M Bu_4NPF_6 in anhydrous DMSO. Bu_4NPF_6 was previously dried in a vacuum oven at 80 °C for 24 h. Due to the insolubility of NDGA in water, this compound was first dissolved in a small amount of DMSO (about 5%) for the studies in aqueous solutions. Solutions were purged with ultra high purity nitrogen (Praxair), which was presaturated with solvent berofe entering the cell. An Autolab PGSTAT 302N potentiostat-galvanostat was used for all the experiments.

Controlled-potential coulometry was carried out in a 75 mL electrolysis cell from Bioanalytical Systems. Reticulated vitreous carbon was used as the working electrode. A platinum wire separated from the bulk of the solution by a frit glass was used as a counter electrode. A reference electrode as mentioned above was used for the voltammetry experiments. Coulometry was carried out at room temperature.

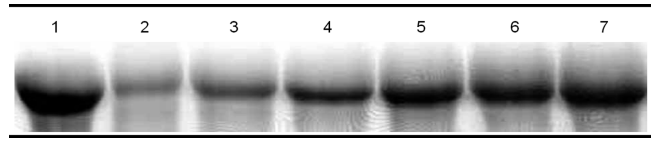

Figure 1. Protective effect of NDGA on BSA oxidation induced by $^{\bullet}OH$ generated by the Fenton reaction. Lane 1, BSA (50 μg); lane 2, BSA (50 μg) + $^{\bullet}OH$; lanes 3−7, BSA (50 μg) + $^{\bullet}OH$ + NDGA. The concentrations of NDGA used are the following (in μM): 10 (lane 3), 20 (lane 4), 30 (lane 5), 40 (lane 6), and 50 (lane 7).

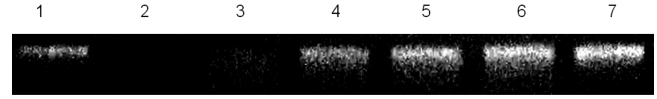

Figure 2. Inhibitory effect of NDGA against oxidative DNA damage induced by $^{\bullet}OH$ generated by the Fenton reaction. Lane 1, DNA (10 μg); lane 2, DNA (10 μg) + $^{\bullet}OH$; lanes 3−6, DNA (10 μg) + $^{\bullet}OH$ + NDGA. The concentrations of NDGA used are the following (in μM): 10 (lane 3), 20 (lane 4), 30 (lane 5), 40 (lane 6), and 50 μM (lane 7).

SCHEME 1

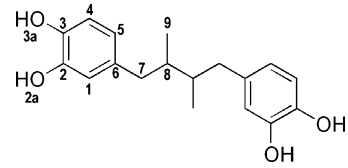

Results and Discussion

Biochemical Studies. Figures 1 and 2 show that NDGA was able to protect, in a concentration-dependent way, BSA and DNA from the $^{\bullet}OH$-induced degradation. The protection was observed starting with the lowest NDGA concentration used (10 μM). These data confirm previous observations about the $^{\bullet}OH$-scavenging effect of NDGA.[12]

Computational Chemistry. The structure of NDGA, as well as the site numbers assigned to each atom, are shown in Scheme 1. Since the pK_a of NDGA is 9.30,[46] its neutral form will be the one prevailing under physiological conditions, and therefore, it is the NDGA form studied in this work.

Different mechanisms can be involved in the reaction of NDGA with $^{\bullet}OH$. According to its structure, at least three of them seem feasible.

SET:

$$NDGA + {}^{\bullet}OH \rightarrow NDGA^{\bullet+} + OH^- \quad (I)$$

HAT:

$$NDGA + {}^{\bullet}OH \rightarrow NDGA(-H)^{\bullet} + H_2O \quad (II)$$

RAF:

$$NDGA + {}^{\bullet}OH \rightarrow NDGA(OH)^{\bullet} \quad (III)$$

SCHEME 2

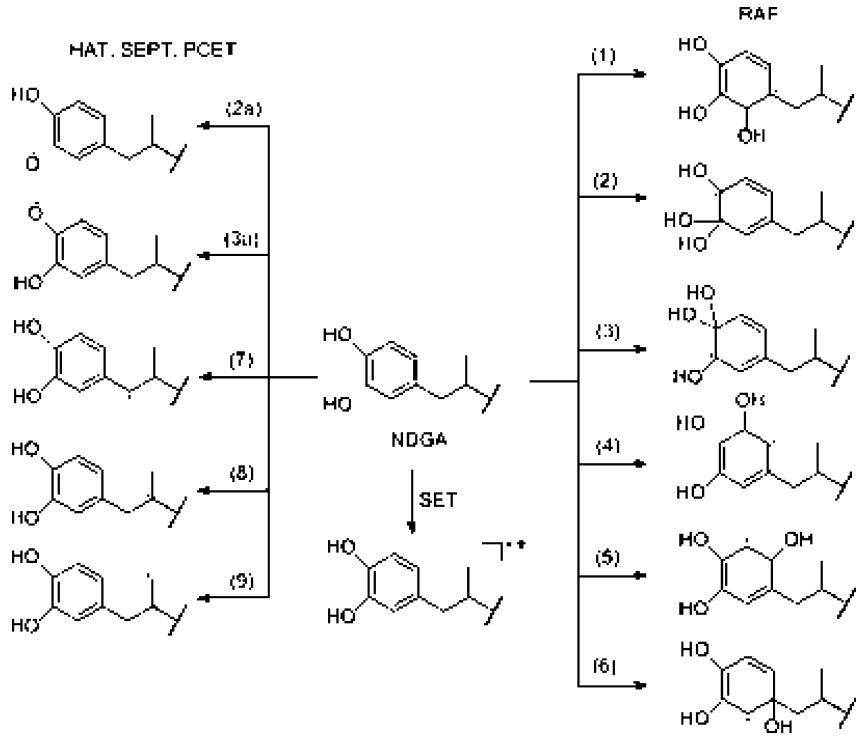

However, SET can occur rapidly followed by, or simultaneously with, proton transfer

$$NDGA^{\bullet+} \rightarrow NDGA(-H)^{\bullet} + H^{+} \qquad (Ia)$$

These processes are referred to as Sequential Electron Proton Transfer (SEPT) and Proton Coupled Electron Transfer (PCET), respectively. Both yield the same radical products as the HAT mechanism. However, the influence of the solvent on their feasibility is expected to be different. While SET and SEPT are likely to occur only on polar environments that promote the solvation of the radical cation, the PCET might also be viable in nonpolar environments since the transfer of the proton and the electron occurs simultaneously in this case, and therefore no charged intermediaries are formed. All the studied products considered for the first step of the NDGA oxidation by $^{\bullet}$OH are shown in Scheme 2.

The optimized structures of the transition states (TS) corresponding to the RAF mechanism are shown in Figure 3. The C···O distance corresponding to the forming bond ranges from 2.026 to 2.088, for TS-1 and TS-5, respectively. No direct relationship was found between the geometrical features of the RAF transition states and the barriers of reaction, indicating that the solvation effects play an important role in the energies of the TSs, relative to that of the isolated reactants.

At this point, we would like to call the reader's attention to the fact that even though it is common to define PCET as a concerted electron proton transfer that is not HAT it has been reported that this is a difficult distinction to make and that HAT can be considered a particular case of PCET reactions.[47] In an attempt to identify if the TS structures shown in Figure 4 actually correspond to HAT or PCET mechanisms, population analyses have been performed. Atomic spin densities on the sites relevant to the studied reactions, and the charge carried by the H atom that is transferred, are reported in Table 1. The coefficients of the natural orbital carrying the unpaired electron indicate that the spin population in transition structures TS-7, TS-8, and TS-9 is concentrated on the two atoms which undergo the H exchange. In addition, a small negative value is found on the H atoms being transferred. This is consistent with a three-center three-

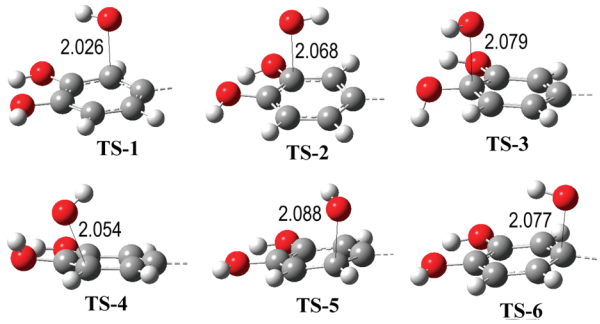

Figure 3. Optimized geometries of the transition states corresponding to $^{\bullet}$OH addition reactions (RAF mechanism). Only the diphenol moiety of NDGA is shown in this figure.

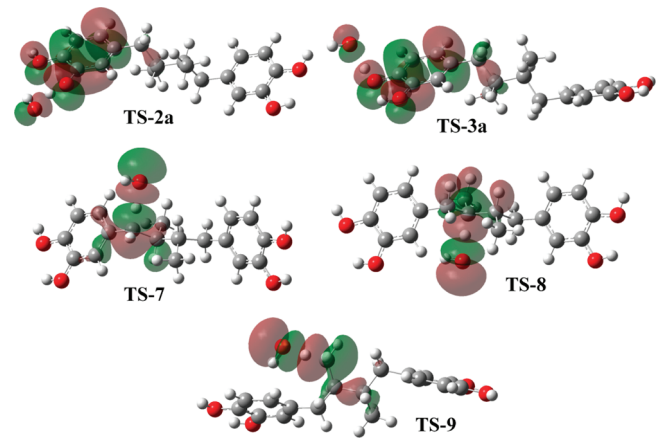

Figure 4. SOMO at PCET (TS-2a and TS-3a) and HAT (TS-7, TS-8, and TS-9) transition structures.

TABLE 1: Atomic Spin Densities and Charge Carried by the Migrating H Atom from Natural Orbital Population Analyses

	spin density		charge	
	water	benzene	water	benzene
TS-2a				
O2a	0.231	0.300		
$H_{transfer}$	−0.005	−0.015	0.565	0.562
O(•OH)	0.022	0.209		
TS-3a				
O3a	0.035	0.077		
$H_{transfer}$	−0.008	−0.013	0.587	0.574
O(•OH)	0.984	0.902		
TS-7				
C7	0.324	0.315		
$H_{transfer}$	−0.038	−0.040	0.262	0.260
O(•OH)	0.704	0.718		
TS-8				
C8	0.305	0.289		
$H_{transfer}$	−0.035	−0.040	0.268	0.263
O(•OH)	0.702	0.732		
TS-9				
C9	0.420	0.398		
$H_{transfer}$	−0.035	−0.043	0.289	0.288
O(•OH)	0.621	0.659		

electron bond and indicates that these TS structures correspond to HAT processes.[48] For transition states TS-2a and TS-3a, on the other hand, the spin population is mainly located on one of the fragments (NDGA or •OH), indicating a PCET mechanism. Another criterion to differentiate between PCET and HAT mechanisms is the charge carried by the H atom that is being transferred. For TS-2a and TS-3a, the migrating H's were found to have substantial positive charge that is typical of proton migrations,[49,50] while the charge on the migrating H's of TS-7, TS-8, and TS-9 is significantly lower. Therefore, according to the charge on the migrating H criterion, TS-2a and TS-3a correspond to PCET processes, while TS-7, TS-8, and TS-9 correspond to HAT reactions. This is in agreement with the previous analyses based on atomic spin densities.

Since it is commonly accepted that the PCET mechanism can be defined as that in which the proton and the electron are transferred between different sets of orbitals,[49] the analysis of the singly occupied molecular orbital (SOMO) of the TS is also used to differentiate between HAT and PCET processes. The SOMO of HAT TSs is expected to have significant density in atomic orbitals oriented along, or nearly along, the transition vector (donor---H---acceptor). The SOMO of PCET TSs, on the other hand, involves p orbitals that are orthogonal to the donor---H---acceptor vector.[49] As the plots in Figure 4 show, the SOMO in TS-7, TS-8, and TS-9 has a node at the migrating H and is mostly localized on the C---H---O vector, which corresponds to HAT transition states. In contrast, the SOMO in TS-2a and TS-3a shows that the p orbital in the H acceptor oxygen is aligned with the transition vector, while the p orbital in the H donor oxygen is orthogonal to it, indicating that the H and the electron transfers take place from different orbitals, i.e., they correspond to the PCET mechanism.

According to all previously discussed criteria, it seems that H atoms in the OH groups of NDGA are transferred to the •OH radical by PCET, while H atoms in the alkyl sites are transferred by HAT.

The transition states for the HAT and PCET mechanisms are shown in Figure 5. TS-2a and TS-3a show hydrogen bond like interactions, which are expected to lower their energies with respect to the other transition states which do not present such an interaction. This structural feature, together with the fact that phenolic hydrogens are more acid than those in alkyl groups, suggests that sites 2a and 3a are the most viable ones for H abstractions.

The Gibbs free energies of reaction (ΔG) for the SET process, which also correspond to the first step of the SEPT mechanism, were found to be 71.21, 14.73, and −5.06 kcal/mol for benzene, DMSO, and water solutions, respectively. These results support the hypothesis mentioned above that the formation of ionic species is only feasible when taking place in highly polar solvents. The ΔG values corresponding to PCET, HAT, and RAF mechanisms are reported in Table 2. The values for HAT reactions also correspond to the overall (cumulative) Gibbs free energy evolution involved in the SEPT and PCET mechanisms. It was found that all the studied reactions are significantly exergonic, regardless of the polarity of the environment. This last aspect influences the exergonicity in an almost negligible way, with ΔG values being only slightly more negative when the reactions occur in polar media for PCET, HAT, and RAF processes, respectively. On the other hand, the influence of the polarity of the solvent on the height of the barriers is significant. PCET, HAT, and RAF barriers become higher as the polarity of the solvent increases, while the barrier of the SET process decreases with the increase of the solvent's polarity (Table 2).

Since the electron transfer processes were found to be endergonic when taking place in benzene and DMSO solutions, they become relevant only in aqueous solution. In this particular case, the barrier of reaction ($\Delta G^{\ddagger}$) was found to be equal to 3.56 kcal/mol. This value is the lowest value among all the computed $\Delta G^{\ddagger}$, suggesting that the mechanisms starting by formation of the radical cation should be the leading ones in the •OH scavenging activity of NGDA in aqueous solution. On the basis of barrier heights alone, PCET from site 3a is expected to be the second major contribution. This channel becomes the one with the lowest barriers in benzene and DMSO, indicating that the polarity of the environment plays an important role on the relative importance of the competing mechanisms. Therefore the kinetics is also expected to be strongly influenced by the polarity of the environment.

The overall rate constant that measures the rate of •OH disappearance has been estimated by summing up the total rate coefficients calculated for all the competing mechanisms

$$k_{\text{overall}} = k_{\text{tot}}^{\text{SET}} + k_{\text{tot}}^{\text{PCET}} + k_{\text{tot}}^{\text{HAT}} + k_{\text{tot}}^{\text{RAF}} \tag{8}$$

with $k_{\text{tot}}^{\text{PCET}}$, $k_{\text{tot}}^{\text{HAT}}$, and $k_{\text{tot}}^{\text{RAF}}$ computed as the sum of the rate constants for the corresponding channels

$$k_{\text{tot}}^{\text{PCET}} = k_{\text{app}}^{\text{PCET-2a}} + k_{\text{app}}^{\text{PCET-3a}} \tag{9}$$

$$k_{\text{tot}}^{\text{HAT}} = k_{\text{app}}^{\text{HAT-7}} + k_{\text{app}}^{\text{HAT-8}} + k_{\text{app}}^{-9} \tag{10}$$

$$k_{\text{tot}}^{\text{RAF}} = k_{\text{app}}^{\text{RAF-1}} + k_{\text{app}}^{\text{RAF-2}} + k_{\text{app}}^{\text{RAF-3}} + k_{\text{app}}^{\text{RAF-4}} + k_{\text{app}}^{\text{RAF-5}} + k_{\text{app}}^{\text{RAF-6}} \tag{11}$$

This approach implies that once a specific channel started it proceeds to completion, independently of the other pathways; i.e., there is no mixing or crossover between different pathways.

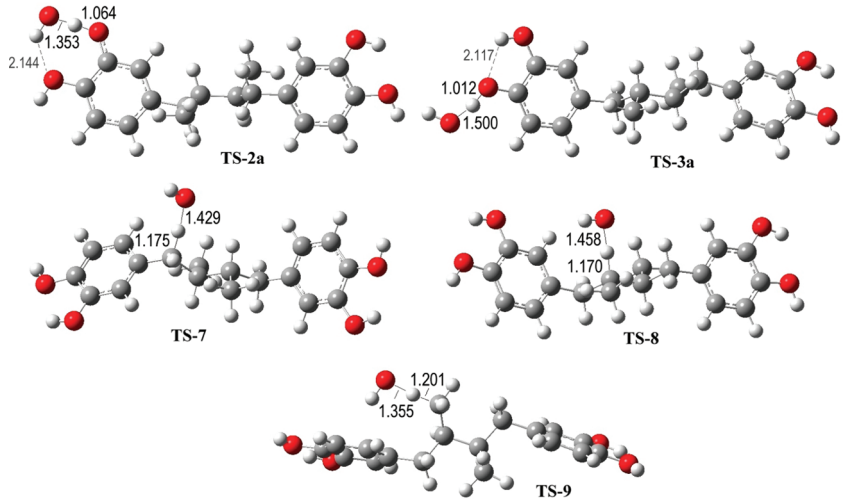

Figure 5. Optimized geometries of the transition states corresponding to HAT (TS-2a and TS-3a) and PCET (TS-7, TS-8, and TS-9) mechanisms.

TABLE 2: Gibbs Free Energies of Reaction (ΔG) and Gibbs Free Energies of Activation ($\Delta G^{\ddagger}$), in kcal/mol, for All the Studied NDGA + •OH Reaction Channels in Solution

	benzene		DMSO		water	
	ΔG	$\Delta G^{\ddagger}$	ΔG	$\Delta G^{\ddagger}$	ΔG	$\Delta G^{\ddagger}$
SET[a]	71.21	95.96	14.73	15.51	−5.06	3.56
PCET-2a	−30.87	2.96	−32.40	5.60	−32.72	8.26
PCET-3a	−39.58	0.96	−38.70	1.89	−37.04	4.15
HAT-7	−31.91	4.71	−32.75	6.35	−34.07	7.68
HAT-8	−24.82	3.31	−25.79	5.48	−27.06	7.25
HAT-9	−19.78	5.26	−20.59	6.94	−22.00	9.21
RAF-1	−13.41	5.40	−11.93	7.42	−11.95	8.99
RAF-2	−17.20	4.08	−16.51	5.41	−16.13	5.77
RAF-3	−20.62	6.26	−18.88	7.53	−17.75	8.50
RAF-4	−15.45	2.24	−13.42	5.11	−13.88	7.79
RAF-5	−15.25	3.65	−13.92	5.48	−14.35	6.58
RAF-6	−12.92	7.51	−11.57	9.10	−10.60	10.39

[a] $\Delta G^{\ddagger}$ values from Marcus theory.

TABLE 3: Rate Constants (k) at 298 K (cm^3 molecule^{-1} s^{-1}) Corresponding to All the Studied Channels of Reaction

	benzene	DMSO	water
SET	–	–	8.95×10^{-12}
PCET-2a	2.83×10^{-12}	8.26×10^{-13}	2.12×10^{-13}
PCET-3a	2.83×10^{-12}	8.59×10^{-13}	1.89×10^{-12}
HAT-7	2.57×10^{-12}	5.77×10^{-13}	1.69×10^{-13}
HAT-8	2.77×10^{-12}	6.80×10^{-13}	1.52×10^{-13}
HAT-9	2.57×10^{-12}	5.64×10^{-13}	3.49×10^{-14}
RAF-1	1.75×10^{-12}	1.28×10^{-13}	1.06×10^{-14}
RAF-2	2.65×10^{-12}	7.21×10^{-13}	1.07×10^{-12}
RAF-3	7.75×10^{-13}	1.09×10^{-13}	2.40×10^{-14}
RAF-4	2.82×10^{-12}	7.70×10^{-13}	7.70×10^{-14}
RAF-5	2.74×10^{-12}	7.07×10^{-13}	4.70×10^{-13}
RAF-6	1.24×10^{-13}	8.79×10^{-15}	1.01×10^{-15}

The calculated rate constants, for all modeled channels of reactions, are reported in Table 3. Since the deprotonation processes from the radical cation are barrierless, the rate constants for SET and SEPT are identical. Therefore, from this point on we will perform our analysis in terms of RAF, SET, PCET, and HAT only. In benzene solution all the HAT and PCET channels were found to be similarly fast. As the polarity of the environment increases, their rates differentiate, and the H transfer from site 3a becomes the fastest one. For •OH addition processes, the rate constants were also found to be influenced by the polarity of the media, except for the addition to site 6,

TABLE 4: Total SET (PCET), HAT (SEPT), and RAF and Overall NDGA + •OH Rate Constants (cm^3 molecule^{-1} s^{-1}) and Branch Ratios (Γ) at 298.15 K[a]

	benzene	DMSO	water
k_{tot}^{SET}	–	–	8.95×10^{-12}
Γ^{SET}	–	–	68.53
k_{tot}^{PCET}	5.66×10^{-12}	1.69×10^{-12}	2.10×10^{-12}
Γ^{PCET}	23.17	28.32	16.09
k_{tot}^{HAT}	7.91×10^{-12}	1.82×10^{-12}	3.56×10^{-13}
Γ^{HAT}	32.38	30.61	2.73
k_{tot}^{RAF}	1.09×10^{-11}	2.44×10^{-12}	1.65×10^{-12}
Γ^{RAF}	44.45	41.07	12.65
$k_{overall}$	2.44×10^{-11}	5.95×10^{-12}	1.31×10^{-11}

[a] $\Gamma_i = (k_i/k_{overall}) \times 100$, with k_i representing the rate constant for each computed mechanism.

which was regularly found as the slowest channel. The fastest channels, through the RAF mechanism, were found to correspond to •OH additions to sites 4 and 5 when the reaction takes place in benzene solution, to sites 2 and 4 when the reaction takes place in DMSO, and to site 2 in aqueous solution. However in the latter case, the SET mechanism is the fastest among all the studied ones.

The total rate coefficients for the different competing mechanisms are shown in Table 4, together with the overall rate coefficient that accounts for the •OH disappearance. The overall rate coefficients show that the NDGA + •OH reaction actually is diffusion-controlled, which supports the efficiency of NDGA as an •OH scavenger. It was found that while in benzene and DMSO solutions HAT, PCET, and RAF mechanisms are about equally fast, and in aqueous solution SET (SEPT) becomes the fastest mechanism of reaction. There is an uncertainty associated with any kinetics calculation. In the particular case of the M05-2X, it has been reported that for a large set of diverse barrier heights the mean error of the method is equal to 1.65 kcal/mol,[51] which is small within the DFT theory. In addition, since all the studied reactions involve the same system (NDGA + •OH) it is expected that any error arising from the method of choice is systematic, and therefore the relative order of the studied mechanism is reliable.

Since there are several channels of reaction that are diffusion controlled, there might be a significant difference between the kinetic site reactivity and the products that are expected to prevail under equilibrium conditions. The direct reaction branching ratios, which are a measurement of the kinetic site

TABLE 5: Branching Ratios (Γ) and Relative Products Population at Equilibrium Conditions (P^{MB}) for Reactions in Aqueous Solution, at 298.15 K[a]

	benzene		DMSO		water	
	Γ	P^{MB}	Γ	P^{MB}	Γ	P^{MB}
NDGA$^{\bullet+}$	—	—	—	—	68.53	∼0
PCET-2a	11.57	∼0	13.88	0.002	1.62	0.07
PCET-3a	11.59	100.00	14.44	99.99	14.45	99.27
HAT-7	10.52	∼0	9.69	0.004	1.30	0.66
HAT-8	11.34	∼0	11.44	∼0	1.16	∼0
HAT-9	10.52	∼0	9.48	∼0	0.27	∼0
RAF-1	7.15	∼0	2.16	∼0	0.08	∼0
RAF-2	10.86	∼0	12.11	∼0	8.21	∼0
RAF-3	3.17	∼0	1.84	∼0	0.18	∼0
RAF-4	11.55	∼0	12.94	∼0	0.59	∼0
RAF-5	11.22	∼0	11.88	∼0	3.60	∼0
RAF-6	0.51	∼0	0.15	∼0	0.01	∼0

[a] $\Gamma_j = (k_j/k_{overall}) \times 100$, with k_j representing the rate constant for each computed channel.

reactivity, together with products population, accounting for the relative distribution of products under equilibrium conditions, are reported in Table 5 for each channel of the studied reactions. The most important point derived from these values is that even though the NDGA radical cation can be formed very rapidly it is expected to evolve equally fast through deprotonation (SEPT), yielding the PCET-3a product. Actually, this product is the one predicted as the main product of reaction, under equilibrium conditions, in all the studied cases.

So far our results indicate that NDGA can react with $^{\bullet}$OH at a diffusion-controlled rate, which supports its activity as a free radical scavenger. However, after its reaction with one $^{\bullet}$OH, is further oxidation possible? If so, it would have relevance to the free radical scavenging activity of NDGA, which then would be able to scavenge not one but two $^{\bullet}$OH. Moreover, it would imply the formation of a closed-shell system, which would end the free radical propagation chain. On the basis of the results for the first oxidation step, we will analyze a possible second step for the oxidation of NDGA by $^{\bullet}$OH taking this product (P-3a) as the starting point. Since the study of the NDGA reaction with the first $^{\bullet}$OH reveals that the most relevant products of reaction are those involving H transfers from the phenolic moieties, we will focus our attention on similar processes for the P-3a + $^{\bullet}$OH reaction (Scheme 3).

According to our results, the elimination of the second hydrogen atom from sites 2a, 2a′, and 3a′ in P-3a are all exergonic reactions (Table 6). The lowest barrier of reaction was systematically found to correspond to the formation of P-3a3a′, regardless of the solvent. Accordingly, this is the path proposed as the fastest one (Table 7). In fact, it was found to be more than one order faster than any of the other two and diffusion-controlled. However, the formed products (P-3a3a′ and P-3a2a′ and P-3a2a) are related by H atom migration equilibria (Scheme 3), which were also found to take place very rapidly (Table 7). Therefore, once P-3a3a′ is formed it can evolve to the others, which in turn may continue reacting.

Since the formation of cyclic structures has been previously proposed for the autoxidation of NDGA,[52] we have also studied the viability of such processes. Formation of cyclic products C1 to C3 (Scheme 3) were found to be exergonic, with their exergonicity increasing with the solvent polarity (Table 8). The formation of C1 was found to be about 1 order of magnitude faster than the formation of C3. The formation of C2 from C1, via tautomeric equilibrium, shows a large exergonicity (−36.1, −34.7, and −27.2 kcal/mol, in benzene, DMSO, and water solutions, respectively). This indicates that C2 should be the most abundant final product of the second oxidation step, under equilibrium conditions.

The mechanism proposed for the oxidation of NDGA by $^{\bullet}$OH is shown in Scheme 4. The final product, at this point, is cycle C2, which in principle might be able to react again with another $^{\bullet}$OH. Therefore, so far we have proven that NDGA can be very effective scavenging at least two $^{\bullet}$OH. Further studies are still needed to test the antioxidant activity of C2. The energetic evolution for the reaction of NDGA with two $^{\bullet}$OH, in terms of Gibbs free energy, is shown in Figure 6. It is expected to occur in a cascade way and very rapidly.

In addition, the UV−vis spectra for the species involved in the proposed mechanism (Scheme 4) have been computed. According to them (Figure 7), NDGA and the species proposed as the main product of reaction (C2), up to this point, absorb at similar wavelength. This implies that, if the proposed mechanism is correct, UV−vis spectra would not show significant changes as the NDGA + $^{\bullet}$OH reaction progresses. This seems to be an important finding because it means that following such changes as indicative of the system evolution might lead to the erroneous conclusion that the NDGA + $^{\bullet}$OH reaction is not feasible.

The reliability of the used methodology, and therefore of the conclusions drawn from the theoretical calculations, is supported by previous studies on the mechanism, kinetic, and spectroscopy of other radical-molecule reactions, where it has been successfully used.[53–66] The computed results are also in line with the experimental data reported in the present work.

Electrochemical Studies. It is well-known that *o*-diphenolic (catecholic) compounds are oxidized to quinones in a one-step, two-electron process forming the corresponding *o*-quinone via the semiquinone forms in a process involving two protons (reaction 11).[67] The proton transfer can be concerted with the electron transfer (PCET process) or can occur in a separate reaction either preceding or following the electron-transfer step (SEPT process). As mentioned above, both mechanisms can produce the same semiquinone radicals as the HAT mechanism; however, since these radicals are highly reactive species, they immediately undergo the diverse kind of fast following chemical reactions or a second electron oxidation to give more stable oxidation products. The reactivity of the semiquinone differs depending on the composition of the reaction media, and for this reason in this work we investigated the electrochemical oxidation of NDGA in both aqueous and nonaqueous solvents, H_2O and DMSO. The insolubility of NDGA in aqueous media may suggest that NDGA acts preferably in a lipophilic region of the biological cell.

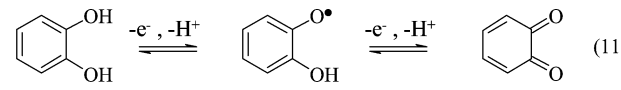

(11)

Figure 8a (black curve) is a representative cyclic voltammogram of NDGA in aqueous solution containing 1.0 M KCl. The voltammogram exhibits an anodic peak, Ia, at 0.57 V. On the reverse scan the counterpart of this peak appears at 0.16 V. Such voltammetric behavior is characteristic of catechol derivatives, and it is attributed to the one-step two-electron redox reaction forming the corresponding *o*-quinone, reaction 11. For NDGA, containing two identical catechol moieties (Scheme 1), a four-electron oxidation process should be expected. However, contrary to our expectation, electro-oxidation of NDGA at 0.62 V consumed an amount of charge corresponding to more than 5 electrons per molecule of NDGA. An exact determination of

SCHEME 3

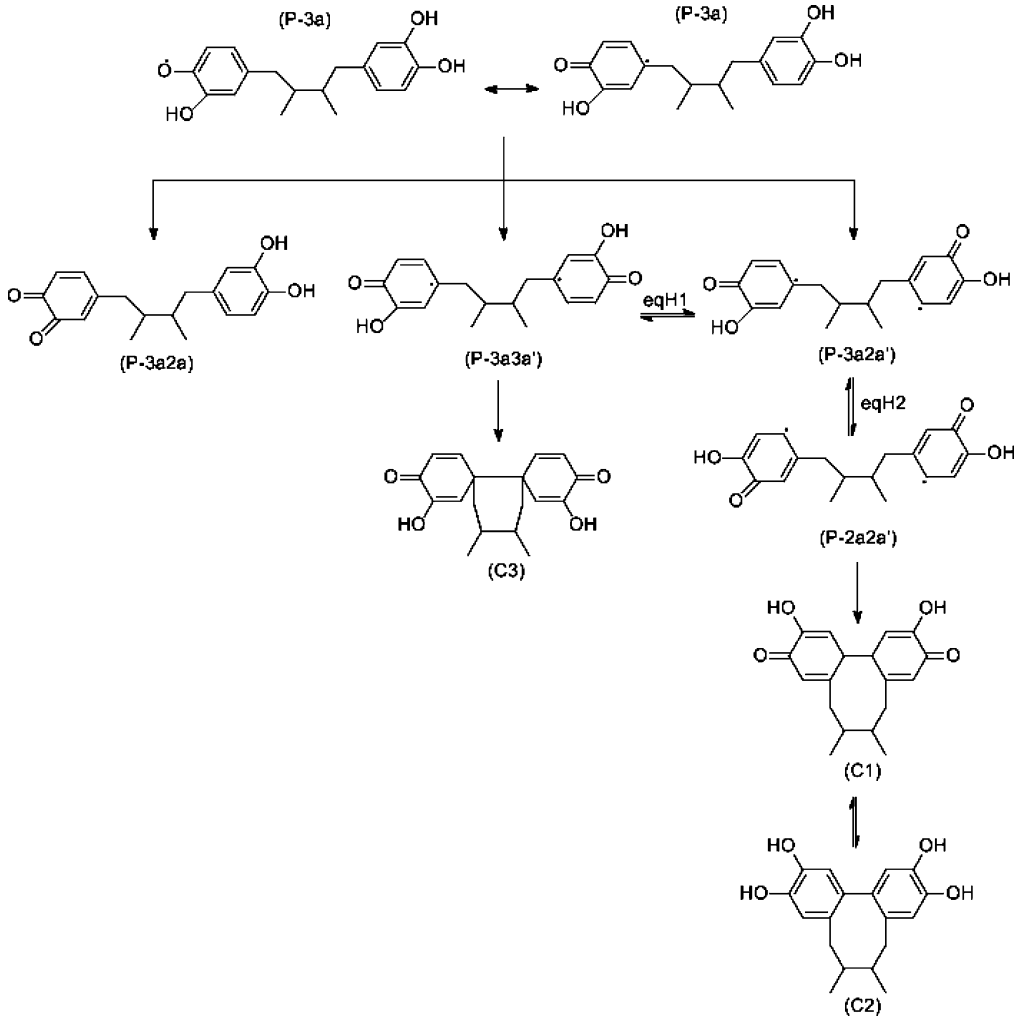

TABLE 6: Gibbs Free Energies of Reaction (ΔG) and Gibbs Free Energies of Activation ($\Delta G^{\ddagger}$), at 298.15 K, for the Second Step of NDGA Oxidation by $^{\bullet}$OH, in kcal/mol

	benzene		DMSO		water	
	ΔG	$\Delta G^{\ddagger}$	ΔG	$\Delta G^{\ddagger}$	ΔG	$\Delta G^{\ddagger}$
P-3a2a	−43.61	14.90	−46.33	15.51	−48.01	17.26
P-3a2a′	−38.28	6.56	−37.39	6.30	−35.77	10.87
P-3a3a′	−38.86	1.58	−38.06	3.11	−36.44	5.08

TABLE 7: Rate Constants (cm^3 molecule^{-1} s^{-1}), at 298.15 K, for the Second Oxidation of NDGA by $^{\bullet}$OH

	benzene	DMSO	water
3a2a	1.28×10^{-19}	4.58×10^{-20}	2.39×10^{-21}
3a2a′	1.56×10^{-13}	1.98×10^{-13}	1.15×10^{-16}
3a3a′	2.82×10^{-12}	8.46×10^{-13}	9.83×10^{-13}
eqH1	2.76×10^{-12}	8.57×10^{-13}	1.90×10^{-12}
eqH2	2.68×10^{-12}	8.55×10^{-13}	1.89×10^{-12}

TABLE 8: Gibbs Free Energies of Reaction (ΔG) and Gibbs Free Energies of Activation ($\Delta G^{\ddagger}$), in kcal/mol, and Rate Constants (k, cm^3 molecule^{-1} s^{-1}) for the Formation of Cycles C1 and C3, at 298.15 K

	C1	C3
Benzene		
ΔG	−3.91	−4.37
$\Delta G^{\ddagger}$	15.59	17.02
k	3.82×10^{-2}	3.47×10^{-21}
DMSO		
ΔG	−5.71	−5.15
$\Delta G^{\ddagger}$	15.67	17.08
k	3.34×10^{-20}	3.13×10^{-21}
Water		
ΔG	−11.40	−6.41
$\Delta G^{\ddagger}$	15.16	16.85
k	7.90×10^{-20}	4.62×10^{-21}

number of electrons transferred was not possible since the charge continued to increase infinitely with time.

In a second electro-oxidation experiment, the electrolysis was stopped after passing a charge equivalent to 2 Faraday per mol of NDGA, and a cyclic voltammogram was recorded. The voltammogram shows that the original peak Ia, corresponding to the oxidation of NDGA, is absent, and a new anodic peak appears at slightly more positive potentials (Figure 8, red curve). This observation indicates the formation of a new product that is slightly more difficult to oxidize than NDGA. As shown in Scheme 3, the possible products of a two-electron oxidation process of NDGA are cyclic compounds C1 to C3, experimentally the product P-3a2a, with only one catecholic ring oxidized would not be feasible since both aromatic rings are equivalent. Formation of compounds C1 to C3 involves the intramolecular dimerization of the initially formed dication diradical. The dimerization of radical cations of phenols and catechols is a well-documented reaction.[68–70] The ionization potential values calculated in water for NDGA 4.86 eV, C1 6.68 eV, C2 5.31 eV, and C3 5.95 eV suggest that the three cyclic compounds

SCHEME 4

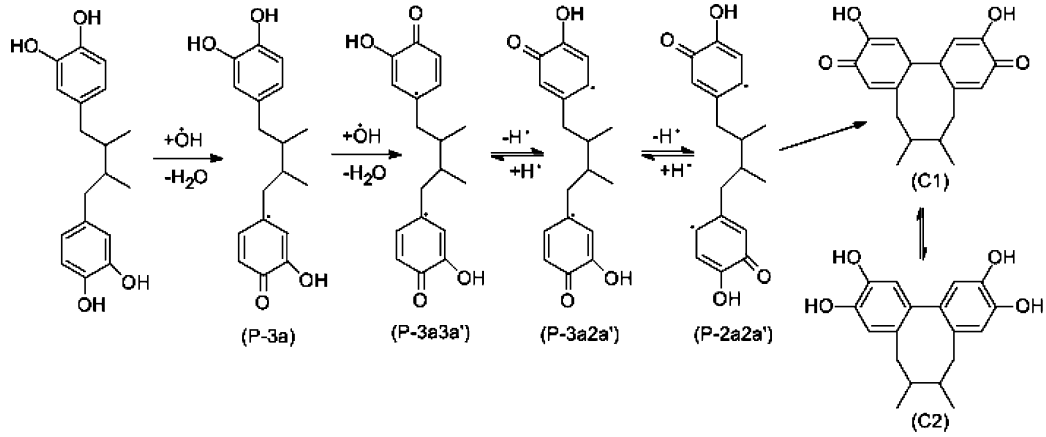

would be oxidized at higher potential than NDGA. On the other hand, by the voltammetric features of the red curve (Figure 8), an oxidation peak with an associated reduction peak, it is possible to assume that the new oxidation product corresponds to a diphenol derivative, such as, for example, C2. This is further supported by the absorption spectra of the electrolyzed solution which showed an absorption band at λ_{max} 280 nm (data not shown) which is in agreement with the calculated spectra for this compound (Figure 7) and with the experimental observation of Billinsky et al.[52] who have recently reported that the cyclic compound C2 exhibits a λ_{max} at 286 nm on the absorption spectra. Some effort was devoted to isolate the products of the electro-oxidation of NDGA. Unfortunately, we did not succeed, probably because the electrochemical oxidation is complicated by polymerization products, as evidenced by the electrode passivation during the electrolysis and by the complexity of the mixture, as revealed by thin layer chromatography.

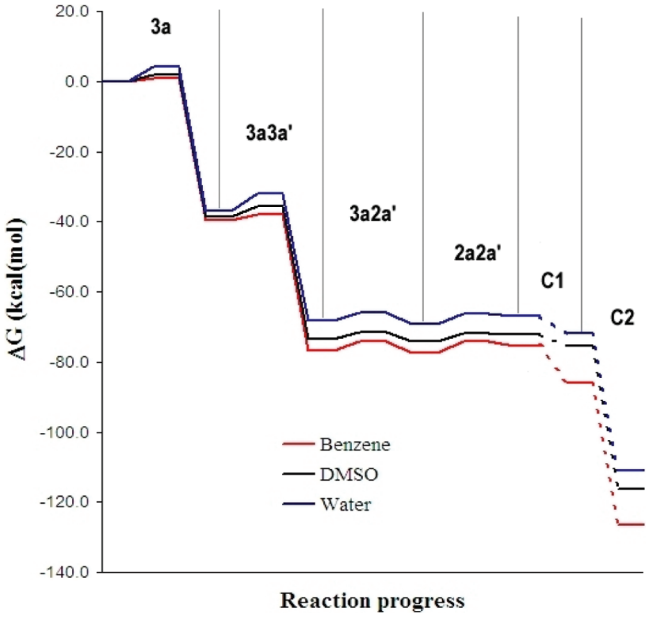

Figure 6. Reaction profile, in terms of Gibbs free energy, for the NDGA oxidation by •OH.

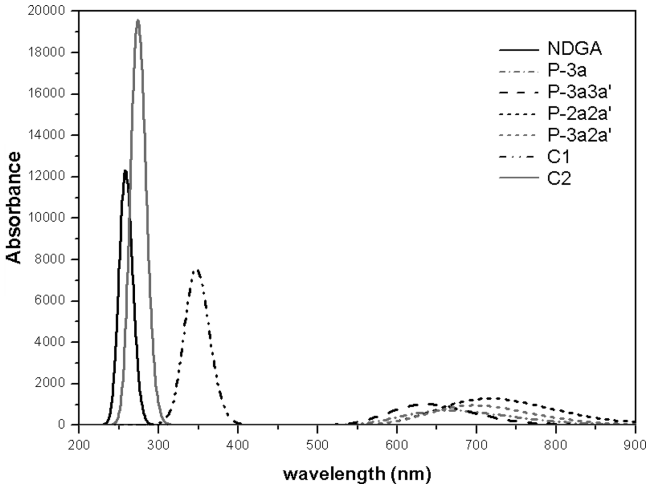

Figure 7. Computed UV−vis spectra of the species involved in the proposed mechanism.

The cyclic voltammogram of NDGA in DMSO containing 0.1 M Bu_4NPF_6 as the supporting electrolyte shows during the first positive-going sweep an anodic wave Ia at 0.25 V accompanied by an associated cathodic peak (Ic) at 0.68 V on the return scan (Figure 9, curve a). The initial negative-going sweep in curve b reveals that the cathodic peak Ic is not observed, and peak Ia was present during the reverse scan (curve b). This behavior clearly shows that the species that is reduced at the potential of peak Ic is not present in the bulk of the solution, but it is generated on the electrode surface by the oxidation of NDGA at the potential of the anodic wave Ia. Similar behavior has been observed for the oxidation of hydroquinone in acetonitrile, and it has been described that under these conditions the oxidation of hydroquinone follows an ECE sequence under a mixed kinetic control by electron and proton

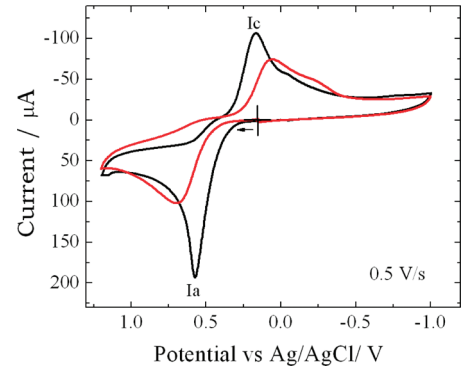

Figure 8. Cyclic voltammograms of 3.84 mM NDGA in 1.0 M KCl at the glassy carbon working electrode, scan rate 0.5 V/s, at room temperature. Before (black curve) and after passing 2 Faraday per mol of NDGA at an oxidation potential of 0.62 V vs $Ag/AgNO_3$ (red curve).

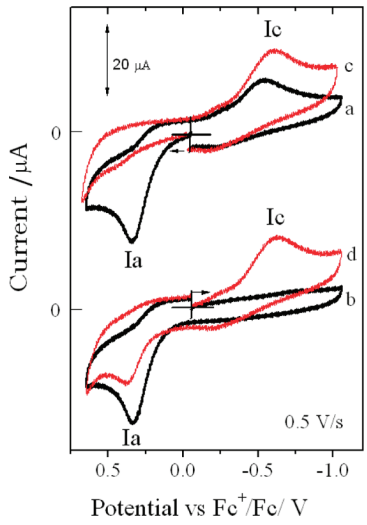

Figure 9. Cyclic voltammograms of 0.58 mM NDGA in 0.1 M Bu_4NPF_6 in DMSO at glassy carbon working electrode, scan rate 0.5 V/s at room temperature. Before (a and b) and after complete electrolysis at 0.53 V vs Fc^+/Fc (c and d).

transfer, E being an electron transfer and C a chemical reaction, that in this case corresponds to a loss of proton.[71]

Electro-oxidation of NDGA in DMSO exhibits different behavior. Controlled-potential coulometry at the potential of peak Ia (0.53 V) consumed about 4 Faraday per mol. As shown in Figure 9, cyclic voltammograms of the electrolyzed solution (curves c and d) correspond to the inverse of those starting with a solution of nonelectrolyzed NDGA. The absence of peak Ia during the initial positive-going scan (curve c) shows that NDGA has been completely oxidized, and no other oxidation peaks were observed when the scan was extended to more positive potentials. The presence of peak Ic during the initial negative-going scan (curve d) is associated with the reduction of the NDGA oxidation product, and the fact that peak Ia is observed only after passing through the peak Ic is evidence that NDGA is being regenerated. This behavior is indicative that both catechol rings in NDGA are transformed to corresponding *o*-benzoquinone and vice versa within a quasireversible two-electron transfer process per catechol unity (reaction 11).

Conclusions

In our study, it was shown that NDGA is able to protect BSA and DNA from the damage induced by •OH. It is proposed that NDGA is an efficient •OH scavenger. It might trap at least two of them, terminating the radical chain propagation. The reaction was found to be very fast; in fact, it is predicted to be diffusion-controlled. The mechanism of the first two steps of the NDGA oxidation by •OH is proposed. The first step is proposed to occur mainly by SEPT, yielding P-3a as the main product of reaction. After a cascade sequential complex reaction the main product of the second step has been identified as C2, as previously proposed by Billinsky et al.[52] This cyclic product is predicted to have a UV−vis spectrum very similar to that of NDGA, making its identification very difficult by this technique. The electrochemical studies performed in water support the formation of C2 as the main product of the reaction.

Acknowledgment. A.G. thanks Laboratorio de Visualización y Cómputo Paralelo at UAM - Iztapalapa for the access to its computer facilities. This work was supported by CONACYT 89641 (O.N.M.-C.) and 51906 (N.A.M.-R.) and by DGAPA IN201910 (J.P.-CH.) and IN203208 (N.A.M.-R.).

References and Notes

(1) Sies, H. *Oxygen Stress*; Academic Press: London, 1985.
(2) Simic, M. G.; Taylor, K. A.; Ward, J. F.; Von Sonntag, C. *Oxygen Radicals in Biology and Medicine*; Plenum Press: New York, 1991.
(3) Davies, K. J. A. *Oxydative Damage and Repair: Chemical, Biological and Medical Aspects*; Pergamon Press: New York, 1991.
(4) Sies, H. *Oxygen Stress-Oxidants and Anti-Oxidants*; Academic Press: London, 1991.
(5) Stadtman, E. R. *Annu. Rev. Biochem.* **1993**, *62*, 797.
(6) Von Sonntag, C. *The Chemical Basis of Radiation Biology*; Taylor & Francis: London, 1987.
(7) (a) Boyd, N. F.; McGuire, V. *Free Radical Biol. Med.* **1991**, *10*, 185. (b) Nelson, R. L. *Free Radical Biol. Med.* **1992**, *12*, 161. (c) Knekt, P.; Reunanen, A.; Takkunen, H.; Aromaa, A.; Heliovaara, M.; Hakuunen, T. *Int. J. Cancer* **1994**, *56*, 379. (d) Omenn, G. S.; Goodman, G. E.; Thornquist, M. D. *N. Engl. J. Med* **1996**, *334*, 1150.
(8) (a) Riemmersma, R. A.; Wood, D. A.; Macityre, C. C. A.; Elton, R. A.; Gey, K. F.; Oliver, M. F. *Lancet* **1991**, *337*, 1. (b) Salonen, J. T.; Nyyssoner, K.; Korpela, H.; Tuomilehto, J.; Seppanen, R.; Salonen, R. *Circulation* **1992**, *86*, 803. (c) Street, D. A.; Comstock, G.; Salkeldy, R.; Klag, M. *Circulation* **1994**, *90*, 1154. (d) Kushi, L. H.; Folsom, A. R.; Prineas, R. J.; Mink, P. J.; Wu, Y.; Bostick, R. *N. Engl. J. Med.* **1996**, *334*, 1156. (e) Stephens, N. G.; Parsons, A.; Schofield, P. M.; Kelly, F.; Cheesman, K.; Mitchisnon, M. J.; Brown, M. J. *Lancet* **1996**, *347*, 781.
(9) (a) Panasenko, O. M.; Nova, T. V.; Azizova, O. A.; Vladimirov, Y. A. *Free Radical Biol. Med.* **1991**, *10*, 137. (b) Steinberg, D. *Circulation* **1991**, *84*, 1421. (c) Janero, D. R. *Free Radical Biol. Med.* **1991**, *11*, 129. (d) Hodis, H. N.; Mack, W. J.; LaBree, L.; Cashin-Hemphill, L.; Sevanian, A.; Johnson, R.; Azen, S. *J. Am. Med. Assoc.* **1995**, *273*, 1849.
(10) (a) Butterfield, D. A.; Hensley, K.; Harris, M.; Mattson, M.; Carney, J. *Biochem. Biophys. Res. Commun.* **1994**, *200*, 710. (b) Hensley, K.; Carney, J. M.; Mattso, M. P.; Aksenova, M.; Harris, M.; Wu, J. F.; Floyd, R. A.; Butterfield, D. A. *Proc. Natl. Acad. Sci. U.S.A.* **1994**, *91*, 3270. (c) Butterfield, D. A.; Martin, L.; Carney, J. M.; Hensley, K. *Life Sci.* **1996**, *58*, 217. (d) Butterfield, D. A. *Chem. Res. Toxicol.* **1997**, *10*, 495. (e) Fay, D. S.; Fluet, A.; Johnson, C. J.; Link, C. D. *J. Neurochem.* **1998**, *71*, 1616.
(11) Arteaga, S.; Andrade-Cetto, A.; Cardenas, R. *J. Ethnopharmol.* **2005**, *98*, 231.
(12) Floriano-Sanchez, E.; Villanueva, C.; Medina-Campos, O. N.; Rocha, D.; Sanchez-Gonzalez, D. J.; Cardenas-Rodriguez, N.; Pedraza-Chaverri, J. *Free Radical Res.* **2006**, *40*, 523.
(13) Ansar, S.; Iqbal, M.; Athar, M. *Carcinogenesis* **1999**, *20*, 599.
(14) Yam-Canul, P.; Chirino, Y. I.; Sánchez-González, D. J.; Martínez-Martínez, C. M.; Cruz, C.; Villanueva, C.; Pedraza-Chaverri, J. *Food Chem. Toxicol.* **2008**, *46*, 1089.
(15) Anjaneyulu, M.; Chopra, K. *Pharmacology* **2004**, *72*, 42.
(16) Nakayama, T.; Hori, K.; Terazawa, K.; Kawakishi, S. *Free Radical Res. Commun.* **1991**, *14*, 173.
(17) Nakayama, T.; Hori, K.; Ogawa, T.; Kawashi, S. *Biosci. Biotechnol. Biochem.* **1992**, *56*, 1162.
(18) Cárdenas-Rodríguez, N.; Guzmán-Beltrán, S.; Medina-Campos, O. N.; Orozco-Ibarra, M.; Massieu, L.; Pedraza-Chaverri, J. *J. Biochem. Mol. Toxicol.* **2009**, *23*, 137.
(19) Kocha, T.; Yamaguchi, M.; Ohtaki, H.; Fukuda, T.; Aoyagi, T. *Biochim. Biophys. Acta* **1997**, *1337*, 319.
(20) Atif, F.; Kaur, M.; Ansari, R. A.; Raisuddin, S. *J. Biochem. Mol. Toxicol.* **2008**, *22*, 202.
(21) Zhao, Y.; Schultz, N. E.; Truhlar, D. G. *J. Chem. Theory Comput.* **2006**, *2*, 364.
(22) Frisch, M. J.; Trucks, G. W.; Schlegel, H. B.; Scuseria, G. E.; Robb, M. A.; Cheeseman, J. R.; Montgomery, Jr., J. A.; Vreven, T.; Kudin, K. N.; Burant, J. C.; Millam, J. M.; Iyengar, S. S.; Tomasi, J.; Barone, V.; Mennucci, B.; Cossi, M.; Scalmani, G.; Rega, N.; Petersson, G. A.; Nakatsuji, H.; Hada, M.; Ehara, M.; Toyota, K.; Fukuda, R.; Hasegawa, J.; Ishida, M.; Nakajima, T.; Honda, Y.; Kitao, O.; Nakai, H.; Klene, M.; Li, X.; Knox, J. E.; Hratchian, H. P.; Cross, J. B.; Bakken, V.; Adamo, C.; Jaramillo, J.; Gomperts, R.; Stratmann, R. E.; Yazyev, O.; Austin, A. J.; Cammi, R.; Pomelli, C.; Ochterski, J. W.; Ayala, P. Y.; Morokuma, K.; Voth, G. A.; Salvador, P.; Dannenberg, J. J.; Zakrzewski, V. G.; Dapprich, S.; Daniels, A. D.; Strain, M. C.; Farkas, O.; Malick, D. K.; Rabuck, A. D.; Raghavachari, K.; Foresman, J. B.; Ortiz, J. V.; Cui, Q.; Baboul, A. G.; Clifford, S.; Cioslowski, J.; Stefanov, B. B.; Liu, G.; Liashenko, A.; Piskorz, P.; Komaromi, I.; Martin, R. L.; Fox, D. J.; Keith, T.; Al-Laham, M. A.; Peng, C. Y.; Nanayakkara, A.; Challacombe, M.; Gill, P. M. W.; Johnson, B.; Chen, W.; Wong, M. W.; Gonzalez, C.; Pople, J. A. *Gaussian 03*, Revision E.01, Gaussian, Inc.: Wallingford, CT, 2004.
(23) Cances, M. T.; Mennucci, B.; Tomasi, J. *J. Chem. Phys.* **1997**, *107*, 3032.
(24) Mennucci, B.; Cances, E.; Tomasi, J. *J. Phys. Chem. B* **1997**, *101*, 10506.
(25) Tomasi, J.; Mennucci, B.; Cances, E. *J. Mol. Struct. (Theochem)* **1999**, *464*, 211.

(26) Okuno, Y. *Chem.—Eur. J.* **1997**, *3*, 210.
(27) Benson, S. W. *The foundations of chemical kinetics*; Malabar, Florida: Krieger, 1982.
(28) Ardura, D.; Lopez, R.; Sordo, T. L. *J. Phys. Chem. B* **2005**, *109*, 23618.
(29) Alvarez-Idaboy, J. R.; Reyes, L.; Cruz, J. *Org. Lett.* **2006**, *8*, 1763.
(30) Alvarez-Idaboy, J. R.; Reyes, L.; Mora-Diez, N. *Org. Biomol. Chem.* **2007**, *5*, 3682.
(31) Galano, A. *J. Phys. Chem. A* **2007**, *111*, 1677.
(32) Galano, A. *J. Phys. Chem. C* **2008**, *112*, 8922.
(33) Galano, A.; Cruz-Torres, A. *Org. Biomol. Chem.* **2008**, *6*, 732.
(34) Galano, A.; Francisco-Márquez, M. *Chem. Phys.* **2008**, *345*, 87.
(35) Mora-Diez, N.; Keller, S.; Alvarez-Idaboy, J. R. *Org. Biomol. Chem* **2009**, *7*, 3682.
(36) Eyring, H. *J. Chem. Phys.* **1935**, *3*, 107.
(37) Evans, M. G.; Polanyi, M. *Trans. Faraday Soc.* **1935**, *31*, 875.
(38) Truhlar, D. G.; Hase, W. L.; Hynes, J. T. *J. Phys. Chem.* **1983**, *87*, 2664.
(39) Eckart, C. *Phys. Rev.* **1930**, *35*, 1303.
(40) Marcus, R. A. *Annu. Rev. Phys. Chem.* **1964**, *15*, 155.
(41) Marcus, R. A. *Rev. Mod. Phys.* **1993**, *65*, 599.
(42) Marcus, R. A. *Pure Appl. Chem.* **1997**, *69*, 13.
(43) Nelsen, S. F.; Blackstock, S. C.; Kim, Y. *J. Am. Chem. Soc.* **1987**, *109*, 677.
(44) Nelsen, S. F.; Weaver, M. N.; Luo, Y.; Pladziewicz, J. R.; Ausman, L. K.; Jentzsch, T. L.; O'Konek, J. J. *J. Phys. Chem. A* **2006**, *110*, 11665.
(45) Collins, F. C.; Kimball, G. E. *J. Colloid Sci.* **1949**, *4*, 425.
(46) Moridani, M. Y.; Siraki, A.; Chevaldina, T.; Scobie, H.; O'Brien, P. J. *Chem. Biol. Interact.* **2004**, *147*, 297.
(47) Mayer, J. M. *Annu. Rev. Phys. Chem.* **2004**, *55*, 363.
(48) Olivella, S.; Anglada, J. M.; Solÿ, A.; Bofill, J. M. *Chem.—Eur. J.* **2004**, *10*, 3404.
(49) Mayer, J. M.; Hrovat, D. A.; Thomas, J. L.; Borden, W. T. *J. Am. Chem. Soc.* **2002**, *124*, 11142.
(50) Turecek, F.; Syrstad, E. A. *J. Am. Chem. Soc.* **2003**, *125*, 3353.
(51) Zhao, Y.; Truhlar, D. G. *Theor. Chem. Acc.* **2008**, *120*, 215.
(52) Billinsky, J. L.; Marcoux, M. R.; Krol, E. S. *Chem. Res. Toxicol.* **2007**, *20*, 1352.
(53) Lundqvist, M.; Eriksson, L. A. *J. Phys. Chem. B* **2000**, *104*, 848-.
(54) Zhang, H. Y.; Sun, Y. M.; Wang, X. L. *Chem.—Eur. J.* **2003**, *9*, 502.
(55) Cao, H.; Pan, X.; Li, C.; Zhou, C.; Denga, F.; Li, T. *Bioorg. Med. Chem. Lett.* **2003**, *13*, 1869.
(56) Leopoldini, M.; Pitarch, I. P.; Russo, N.; Toscano, M. *J. Phys. Chem. A* **2004**, *108*, 92.
(57) Navarrete, M.; Rangel, C.; Corchado, J. C.; Espinosa-Garcia, J. *J. Phys. Chem. A* **2005**, *109*, 4777.
(58) Trouillas, P.; Marsal, P.; Siri, D.; Lazzaroni, R.; Duroux, J. L. *Food Chem.* **2006**, *97*, 679.
(59) Trouillas, P.; Marsal, P.; Svobodova, A.; Vostalova, J.; Gazak, R.; Hrbac, J.; Sedmera, P.; Kren, V.; Lazzaroni, R.; Duroux, J. L.; Walterova, D. *J. Phys. Chem. A* **2008**, *112*, 1054.
(60) Francisco-Márquez, M.; Galano, A. *J. Phys. Chem. B* **2009**, *113*, 4947.
(61) Galano, A.; Alvarez-Idaboy, J. R. *Org. Lett.* **2009**, *11*, 5114.
(62) Galano, A.; Francisco-Márquez, M. *J. Phys. Chem. B* **2009**, *113*, 16077.
(63) Galano, A.; Álvarez-Diduk, R.; Ramírez-Silva, M. T.; Alarcón-Ángeles, G.; Rojas-Hernández, A. *Chem. Phys.* **2009**, *363*, 13.
(64) Guzman, R.; Santiago, C.; Sanchez, M. *J. Mol. Struct.* **2009**, *935*, 110.
(65) Anouar, E.; Kosinova, P.; Kozlowski, D.; Mokrini, R.; Duroux, J. L.; Trouillas, P. *Phys. Chem. Chem. Phys.* **2009**, *11*, 7659.
(66) Dhaouadi, Z.; Nsangou, M.; Garrab, N.; Anouar, E. H.; Marakchi, K.; Lahmar, S. *J. Mol. Struct. THEOCHEM* **2009**, *904*, 35.
(67) Friedman, M. *J. Agric. Food Chem.* **1997**, *45*, 1523.
(68) Hotta, H.; Sakamoto, H.; Nagano, S.; Osakai, T.; Tsujino, Y. *Biochim. Biophys. Acta* **2001**, *1526*, 159.
(69) Hotta, H.; Ueda, M.; Nagano, S.; Tsujino, Y.; Koyama, J.; Osakai, T. *Anal. Biochem.* **2002**, *303*, 66.
(70) Nematollahi, D.; Golabi, S. M. *J. Electroanal. Chem.* **2000**, *481*, 208.
(71) Astudillo, P. D.; Tiburcio, J.; González, F. J. *J. Electroanal. Chem.* **2007**, *604*, 57.

JP912001C